Studia Geotechnica et Mechanica
Volume 47 Issue 4 · pp. 1–14 · DOI: 10.2478/sgem-2025-0021

Studia Geotechnica et Mechanica

Optimization of the dimensions of a tapered thin-walled cantilever, aimed at reaching a maximum critical buckling load

Research Article

Józef Szybiński*, Piotr Ruta

Wrocław University of Science and Technology, Faculty of Civil Engineering, Wrocław, Poland

Received 12 May 2025; Accepted 03 September 2025

Abstract: The aim of this research was to determine the optimal dimensions of a tapered, bisymmetric, thin-walled, I-shaped cantilever for which, at a constant mass, the critical load causing the buckling of the beam reaches the maximum value. Optimal solutions were sought in a discrete set of admissible values of the taper coefficients of the I-bar's web and/or flanges. A model of a thin-walled bar with an open cross-section, whose mathematical description was derived on the basis of the momentless theory of shells, was used to analyse the considered problem described by a system of four coupled differential equations with variable coefficients. The equations were solved using Chebyshev series of the first kind to approximate the generalized displacement functions, and the recurrence algorithm presented in earlier publications by the author(s). A tapered cantilever with a bisymmetric cross-section, subjected to the action of a uniformly distributed load, was analysed. The load can be applied to the I-bar's upper flange or to its lower flange, or it can act in the centre of the web. The obtained critical load values were compared with those obtained using the finite element method and the commercial Sofistik software. In the set of linearly tapered cantilevers with a bisymmetric double-tee cross section, the cantilevers with the highest taper coefficients of the web and the flanges (the free end having the smallest possible dimensions) were found to be optimal (in their case, at a constant mass, the critical buckling load reaches its maximum value).

Keywords: *stability • thin-walled beam • optimization • nonprismatic*

1. Introduction

Analyses of the thin-walled elements of bar structures have been conducted by many authors, as evidenced by the extensive literature on this subject. Andrade and Camotim [1] derived differential equations for the analysis of the lateral torsional buckling (LTB) of monosymmetric thin-walled beams with a tapered cross section. The derived equations were solved using the Rayleigh–Ritz method. The LTB of simply supported I-beams and cantilever I-beams, both with a tapered web, was analysed. The results were compared with those reported by other authors. The LTB problem was also the subject of study by Benyamina et al. [2], who derived nonlinear equilibrium equations and used the Ritz method to solve them. Bisymmetric thin-walled beams with tapered webs were analysed. The results were compared with those obtained using the finite element method (FEM). Andrade et al. [3] presented a one-dimensional model enabling the analysis of the LTB of nonprismatic thin-walled beams with a monosymmetric open cross section. I-shaped thin-walled beams and cantilever beams, both with linearly tapered webs, were analysed. In order to verify the model, the numerical results obtained using this model were compared with those obtained by FEM. Asgarian et al. [4] presented a nonprismatic thin-walled beam model and used it to analyse the LTB stability of nonprismatic thin-walled beams with any cross sections and various support schemes. The differential equations with variable coefficients, derived using Hamilton's principle, were solved using the power series method. In order to verify the efficacy of the method used, the results were compared with those reported by other authors and with those obtained using FEM. Branford [5] used the latter method to analyse

* *E-mail: jozef.szybinski@pwr.edu.pl*

Open Access. © 2025 Józef Szybiński and Piotr Ruta, published by Wroclaw University of Science and Technology
This work is licensed under the Creative Commons Attribution-NonCommercial-NoDerivs 4.0 License.

the LTB of monosymmetric nonprismatic I-beams under any load and any support conditions. The obtained results were compared to those reported in the literature on the subject. Challamel et al. [6] analysed the LTB of cantilever beams with a linearly tapered web. An analytical solution to the problem was obtained in the form of hypergeometric functions. Also, a solution to the cantilever shape optimization problem was presented, assuming the maximum warping resistance of the cantilever as the optimization criterion. The effect of shear strains on the buckling of nonprismatic thin-walled beams with a bisymmetric cross section was studied by Osmani and Meftah [7]. Beams with an open and closed cross-section, loaded with a combination of forces causing bending and axial deformations, were analysed. The Ritz method was used to solve the nonlinear equilibrium equations. The critical load determined using the proposed method was shown to agree with the results yielded by FEM (ABAQUS). Raftoyiannis and Adamakos [8] developed a numerical procedure for determining the critical load causing the LTB of I-beams with nonprismatic webs. The obtained results were compared with those reported in the literature on the subject. Rezaiee-Pajand et al. [9] studied the LTB of a nonprismatic thin-walled beam at variable material parameters (the elasticity modulus and the rigidity modulus) in both the longitudinal and transverse directions. Beams with a symmetric double-tee cross-section and a linearly variable depth of the web were analysed. The sought total displacement functions were approximated with sine trigonometric series. Soltani [10] presented a method of analysing the LTB of nonprismatic composite beams with a symmetric double-tee cross section. The problem was solved using the Ritz method. In order to demonstrate the accuracy of the proposed method, the results were compared with those obtained by FEM (ANSYS) in which shell elements were used for the approximation. Soltani and Asgarian [11,12] used the FEM and the differential quadrature method to analyse the LTB of bisymmetric nonprismatic beams with variable (along the length) material parameters. Beams with various load diagrams were analysed. Energy methods were used to derive equilibrium equations. The effect of factors such as material property variation along the bar length, bending moment gradient variation, or the transverse load application level on LTB was studied. The LTB of beams with variable material parameters along the length was investigated by Soltani et al. [13]. Pinned nonprismatic I-beams with material parameters (continuously) varying along the length were analysed using FEM. Soltani et al. [14] used the finite difference method to solve the LTB problem for thin-walled beams with any load diagram. In order to verify the applied method, the results were compared with those obtained by FEM, in which shell elements were used for approximation. Zhang and Tong [15] analysed the LTB of I-beams with a nonprismatic web. Using Vlasov's assumptions and variational methods, they derived equations describing the behaviour of this type of beam. It was shown, among other things, that the FEM using prismatic beam elements for approximation may yield results significantly different from the results obtained using other methods. El-Mahdy and El-Saadawy [16] created a three-dimensional thin-walled beam model in ANSYS. They used this model to analyse the effect of the variable ratio of the compression flange dimensions to the tension flange dimensions (at a fixed quantity of material used) on the optimal performance characteristics of the system, i.e. on the beam's load-bearing capacity considering the LTB.

In the present study, displacement differential equations describing the global buckling problem for a thin-walled nonprismatic bar with a bisymmetric cross section, subjected to a uniformly distributed load, are derived using the minimal elastic strain energy principle. The recurrence algorithm described in earlier papers by the author(s) [17–25] is used to solve the system of displacement differential equations with variable coefficients. In this algorithm, Chebyshev series of the first kind are employed to approximate the generalized displacement functions. A tapered cantilever with a bisymmetric cross-section, subjected to a uniformly distributed load, is analysed. The load can be applied to the I-beam's upper flange, its lower flange, or it can act in the web's centre. The determined critical load values are compared with those obtained using FEM and the commercial Sofistik [26] software. The obtained results show that among the linearly tapered cantilevers with a bisymmetric double-tee cross section, cantilevers with the highest web and flanges taper coefficients (the free end having the smallest possible dimensions, while the fixed end has the largest possible dimensions) are the optimal ones (in their case, at a constant mass, the critical load causing the LTB reaches its maximum value. This finding can be surprising as it indicates that the cantilever's "stronger" part (at the fixed end) contributes considerably more to an increase in critical load than its "weaker" part (at the free end).

2. Mathematical description of the bar model

A model presented previously [23,25] was used in this study to describe a thin-walled beam with an open cross-section. The model was based on the momentless theory of shells and

Vlasov's assumptions, and it is a generalization of Wilde's model [27]. Here, only the essential equations describing the model are quoted, specifically for the case when the system's cross sections are bisymmetric. The detailed derivation of the general equations for any cross-section can be found from the previous study [23]. Figure 1 shows the coordinate systems used in the description of the considered model.

Under the adopted assumptions, the displacement of any point of the thin-walled bar is given by the following formula:

$$\begin{aligned}\boldsymbol{u} &= U_x\boldsymbol{e}_x + U_y\boldsymbol{e}_y + U_z\boldsymbol{e}_z \\ &= u_x(x,s)\boldsymbol{e}_x + [u_y(x) - z(x,s)\theta(x)]\boldsymbol{e}_y \\ &\quad + [u_z(x) + y(x,s)\theta(x)]\,\boldsymbol{e}_z,\end{aligned} \tag{1}$$

where $\theta(x)$ is the angle of rotation relative to the axis defined by the points with coordinates $(C_y(x) = 0,\ C_z(x) = 0)$ specifying the shear centre; $u_y(x), u_z(x)$ are the cross-section displacement components in the shear centre, measured along the axis of the global coordinate system, $u_x(x, s)$ is a measure of cross-sectional displacement along the x-axis, which takes into account warpings relative to the plane x = const (Figure 2).

As shown in previous studies [23,27], the use of Vlasov's assumptions ($\gamma_{x\,s} = 0$) leads to the following formula for displacements u_x:

$$u_x = u_{ox} - yu_{y,x} - zu_{z,x} - \omega\theta_{,x}, \tag{2}$$

where $u_{ox} = u_{ox}(x)$ is an integration constant independent of s, and $\omega = \omega(x, s)$ is a sectorial coordinate described by the relationship

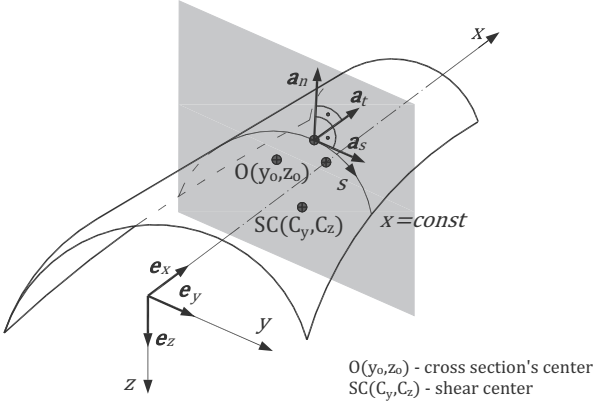

Figure 1. Coordinate system and local basis vectors for a nonprismatic thin-walled beam.
Source: Author's contribution.

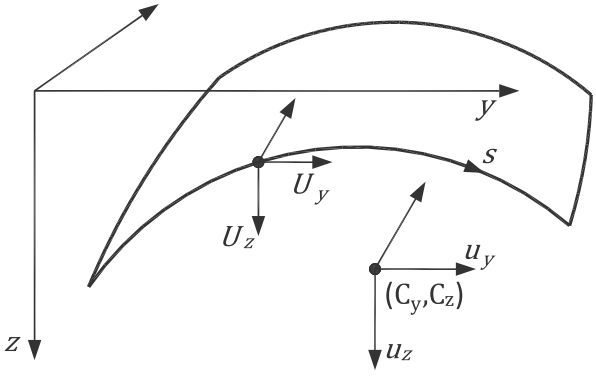

Figure 2. Description of displacements for the cross-section.
Source: Author's contribution.

$$\omega(x,s) = \int[-zy_{,s} + yz_{,s}]\mathrm{d}s. \tag{3}$$

The linear and nonlinear components of the strain tensor are defined by the respective formulas

$$\gamma_{\alpha\beta} = \frac{1}{2}(\mathbf{a}_\alpha \circ \mathbf{u}_{,\beta} + \mathbf{a}_\beta \circ \mathbf{u}_{,\alpha}), \tag{4}$$

$$\gamma^{nl}_{xx} = \frac{1}{2}(\mathbf{u}_{,x} \circ \mathbf{u}_{,x}), \quad \gamma^{nl}_{xs} = \frac{1}{2}(\mathbf{u}_{,x} \circ \mathbf{u}_{,s}). \tag{5}$$

Substituting the displacement function $\mathbf{u}(x,\ s)$, defined in formula (1), into formulas (4) and (5), the appropriate derivatives were calculated and laborious transformations were carried out and the following formulas were obtained for:

- Linear strains:

$$\gamma_{xx} = u_{ox,x} - yu_{y,xx} - zu_{z,xx} - \omega\theta_{,xx} - \psi\theta_{,x}, \tag{6}$$

where

$$\psi = \omega_{,x} + y_{,x}z - z_{,x}y. \tag{7}$$

- Nonlinear strains:

$$\begin{aligned}\gamma^{nl}_{xx} = \frac{1}{2}(&\alpha^{x,1}_{x,1}u^2_{ox,x} + \alpha^{y,1}_{y,1}u^2_{y,x} + \alpha^{y,2}_{y,2}u^2_{y,xx} + \alpha^{z,1}_{z,1}u^2_{z,x} + \alpha^{z,2}_{z,2}u^2_{z,xx} \\ &+ \alpha^{\theta}_{\theta}\theta^2 + \alpha^{\theta,1}_{\theta,1}\theta^2_{,x} + \alpha^{\theta,2}_{\theta,2}\theta^2_{,xx}) + \alpha^{y,1}_{x,1}u_{ox,x}u_{y,x} \\ &+ \alpha^{y,2}_{x,1}u_{ox,x}u_{y,xx} + \alpha^{z,1}_{x,1}u_{ox,x}u_{z,x} + \alpha^{z,2}_{x,1}u_{ox,x}u_{z,xx} \\ &+ \alpha^{\theta,1}_{x,1}u_{ox,x}\theta_{,x} + \alpha^{\theta,2}_{x,1}u_{ox,x}\theta_{,xx} + \alpha^{z,1}_{y,1}u_{y,x}u_{z,x} \\ &+ \alpha^{z,2}_{y,2}u_{y,xx}u_{z,xx} + \alpha^{y,2}_{y,1}u_{y,x}u_{y,xx} + \alpha^{z,2}_{y,1}u_{y,x}u_{z,xx} \\ &+ \alpha^{y,2}_{z,1}u_{z,x}u_{y,xx} + \alpha^{z,2}_{z,1}u_{z,x}u_{z,xx} + \alpha^{\theta}_{y,1}u_{y,x}\theta + \alpha^{\theta,1}_{y,1}u_{y,x}\theta_{,x} \\ &+ \alpha^{\theta,2}_{y,1}u_{y,x}\theta_{,xx} + \alpha^{\theta,1}_{y,2}u_{y,xx}\theta_{,x} + \alpha^{\theta,2}_{y,2}u_{y,xx}\theta_{,xx} + \alpha^{\theta}_{z,1}u_{z,x}\theta \\ &+ \alpha^{\theta,1}_{z,1}u_{z,x}\theta_{,x} + \alpha^{\theta,2}_{z,1}u_{z,x}\theta_{,xx} + \alpha^{\theta,1}_{z,2}u_{z,xx}\theta_{,x} \\ &+ \alpha^{\theta,2}_{z,2}u_{z,xx}\theta_{,xx} + \alpha^{\theta,1}_{\theta}\theta\theta_{,x} + \alpha^{\theta,2}_{\theta,1}\theta_{,x}\theta_{,xx},\end{aligned} \tag{8}$$

$$\gamma_{xs}^{nl} = \frac{1}{2}(\zeta_{y,1}^{y,1}u_{y,x}^2 + \zeta_{z,1}^{z,1}u_{z,x}^2 + \zeta_{\theta}^{\theta}\theta^2 + \zeta_{\theta,1}^{\theta,1}\theta_{,x}^2) + \zeta_{x,1}^{y,1}u_{ox,x}u_{y,x} + \zeta_{x,1}^{z,1}u_{ox,x}u_{z,x} + \zeta_{x,1}^{\theta,1}u_{ox,x}\theta_{,x} + \zeta_{y,1}^{y,2}u_{y,x}u_{y,xx} + \zeta_{y,1}^{z,2}u_{y,x}u_{z,xx} + \zeta_{y,1}^{z,1}u_{y,x}u_{z,x} + \zeta_{y,2}^{z,1}u_{y,xx}u_{z,x} + \zeta_{z,1}^{z,2}u_{z,x}u_{z,xx} + \zeta_{y,1}^{\theta}u_{y,x}\theta + \zeta_{y,1}^{\theta,1}u_{y,x}\theta_{,x} + \zeta_{y,1}^{\theta,2}u_{y,x}\theta_{,xx} + \zeta_{y,2}^{\theta,1}u_{y,xx}\theta_{,x} + \zeta_{z,1}^{\theta}u_{z,x}\theta + \zeta_{z,1}^{\theta,1}u_{z,x}\theta_{,x} + \zeta_{z,1}^{\theta,2}u_{z,x}\theta_{,xx} + \zeta_{z,2}^{\theta,1}u_{z,xx}\theta_{,x} + \zeta_{\theta}^{\theta,1}\theta\theta_{,x} + \zeta_{\theta,1}^{\theta,2}\theta_{,x}\theta_{,xx}. \quad (9)$$

The coefficients $\alpha_{p,i}^{q,j}$, $\zeta_{p,i}^{q,j}$ occurring in (8) and (9) are defined by the formulas:

$$\begin{aligned}
&\alpha_{x,1}^{x,1} = 1 \quad \alpha_{y,1}^{y,1} = 1 + y_{,x}^2 \quad \alpha_{z,1}^{z,1} = 1 + z_{,x}^2 \quad \alpha_{y,2}^{y,2} = y^2\\
&\alpha_{z,2}^{z,2} = z^2\\
&\alpha_{\theta}^{\theta} = (y_{,x})^2 + (z_{,x})^2 \quad \alpha_{\theta,1}^{\theta,1} = (\omega_{,x})^2 + y^2 + z^2 \quad \alpha_{\theta,2}^{\theta,2} = \omega^2\\
&\alpha_{x,1}^{y,1} = -y_{,x} \quad \alpha_{x,1}^{y,2} = -y \quad \alpha_{x,1}^{z,1} = -z_{,x} \quad \alpha_{x,1}^{z,2} = -z\\
&\alpha_{x,1}^{\theta,1} = -\omega_{,x} \quad \alpha_{x,1}^{\theta,2} = -\omega\\
&\alpha_{y,1}^{z,1} = y_{,x}z_{,x} \quad \alpha_{y,1}^{z,2} = y_{,x}z \quad \alpha_{z,1}^{y,2} = yz_{,x} \quad \alpha_{y,2}^{z,2} = yz\\
&\alpha_{y,1}^{y,2} = yy_{,x} \quad \alpha_{z,1}^{z,2} = zz_{,x}\\
&\alpha_{y,1}^{\theta,2} = y_{,x}\omega \quad \alpha_{z,1}^{\theta,2} = z_{,x}\omega \quad \alpha_{y,1}^{\theta} = -z_{,x} \quad \alpha_{z,1}^{\theta} = y_{,x}\\
&\alpha_{y,1}^{\theta,1} = y_{,x}\omega_{,x} - z \quad \alpha_{z,1}^{\theta,1} = z_{,x}\omega_{,x} + y\\
&\alpha_{y,2}^{\theta,1} = y\omega_{,x} \quad \alpha_{z,2}^{\theta,1} = z\omega_{,x} \quad \alpha_{y,2}^{\theta,2} = y\omega \quad \alpha_{z,2}^{\theta,2} = z\omega\\
&\alpha_{\theta}^{\theta,1} = z_{,x}z + y_{,x}y \quad \alpha_{\theta,1}^{\theta,2} = \omega_{,x}\omega,
\end{aligned} \quad (10)$$

$$\begin{aligned}
&\zeta_{y,1}^{y,1} = y_{,x}y_{,s} \quad \zeta_{z,1}^{z,1} = z_{,x}z_{,s}\\
&\zeta_{\theta}^{\theta} = y_{,x}y_{,s} + z_{,x}z_{,s} \quad \zeta_{\theta,1}^{\theta,1} = \omega_{,x}\omega_{,s}\\
&\zeta_{x,1}^{y,1} = -\frac{1}{2}y_{,s} \quad \zeta_{x,1}^{z,1} = -\frac{1}{2}z_{,s} \quad \zeta_{x,1}^{\theta,1} = -\frac{1}{2}\omega_{,s}\\
&\zeta_{y,1}^{\theta} = -\frac{1}{2}z_{,s} \quad \zeta_{z,1}^{\theta} = \frac{1}{2}y_{,s}\\
&\zeta_{y,1}^{y,2} = \frac{1}{2}yy_{,s} \quad \zeta_{z,2}^{y,1} = \frac{1}{2}zy_{,s} \quad \zeta_{y,1}^{z,1} = \frac{1}{2}(y_{,x}z_{,s} + z_{,x}y_{,s})\\
&\zeta_{y,2}^{z,1} = \frac{1}{2}yz_{,s} \quad \zeta_{z,1}^{z,2} = \frac{1}{2}zz_{,s}\\
&\zeta_{y,1}^{\theta,1} = \frac{1}{2}(y_{,x}\omega_{,s} + \omega_{,x}y_{,s}) \quad \zeta_{z,1}^{\theta,1} = \frac{1}{2}(z_{,x}\omega_{,s} + \omega_{,x}z_{,s})\\
&\zeta_{y,1}^{\theta,2} = \frac{1}{2}\omega y_{,s} \quad \zeta_{z,1}^{\theta,2} = \frac{1}{2}\omega z_{,s}\\
&\zeta_{y,2}^{\theta,1} = \frac{1}{2}y\omega_{,s} \quad \zeta_{z,2}^{\theta,1} = \frac{1}{2}z\omega_{,s} \quad \zeta_{\theta}^{\theta,1} = \frac{1}{2}(yy_{,s} + zz_{,s})\\
&\zeta_{\theta,1}^{\theta,2} = \frac{1}{2}\omega\omega_{,s}.
\end{aligned} \quad (11)$$

The coefficients $\alpha_{p,i}^{q,j}$, $\zeta_{p,i}^{q,j}$ in formulas (8) and (9) are the multipliers of products $\partial_x^i u_p \cdot \partial_x^j u_q$, respectively, where $u_r = u_{ox}, u_y, u_z, \theta$.

Using the constitutive equations [23,27] and taking into account the fact that in the considered case, $\gamma_{xs} = \gamma_{ss} = 0$, the stress n^{xx} can be written in the form

$$n^{xx} = E'g(1 + \beta^2)^{-2}\gamma_{xx}, \quad (12)$$

where $E' = E/1 - \nu^2$, ν is the Poisson's ratio, E is the Young's modulus, and g is the wall thickness. As it was assumed that $\gamma_{xs} = \gamma_{ss} = 0$, the actual forces n^{xs} cannot be determined from the constitutive relations, i.e. from the strain–stress relations given above. Forces n^{xs} should be determined from the equilibrium equation $n^{x\alpha}|_{\alpha} = 0$. Since the metric tensor for the considered coordinate system is known, one can determine the Christoffel symbols and the covariant derivatives. In the special case when $\gamma = 0$, i.e. the coordinate system is orthogonal (as in the case of I-beams), the equation reduces to the form [27]

$$\left((1 + \beta^2)^{\frac{3}{2}}n^{xs}\right)_{,s} + (1 + \beta^2)^{\frac{1}{2}}((1 + \beta^2)n^{xx})_{,x} = 0. \quad (13)$$

As n^{xx} is known, the above equality can be easily integrated, where one obtains

$$n^{xs} = -(1 + \beta^2)^{-\frac{3}{2}}\int_{s_-}^{s}(1 + \beta^2)^{\frac{1}{2}}((1 + \beta^2)n^{xx})_{,x}. \quad (14)$$

It appears from this equation that when the change in the cross section is so small that one can assume $1 + \beta^2 \approx 1$, the equation reduces to an equation describing the relationship for a prismatic bar.

3. Derivation of displacement equations describing the buckling problem

A system of displacement equations describing the buckling problem (a second-order theory problem) was derived from the minimal potential energy principle by calculating the first-order variation of this energy:

$$\delta(U_S - U_0 - W) = \delta U_S - \delta U_0 - \delta W = 0, \quad (15)$$

where U_S is the linear part of the potential energy of the elastic strain, U_0 is the potential energy generated by the initial stress, and W is the work of the external load.

The potential energy of the elastic strain is expressed by the formula:

$$U_S = \frac{1}{2}\iint E'\gamma_{xx}^2 \mathrm{d}A^* \mathrm{d}x + \frac{1}{2}\int_{-a}^{a} \mathrm{GI}_s(\theta_{,x})^2 \mathrm{d}x, \tag{16}$$

where GI_s is stiffness in Saint-Venant torsion and $\mathrm{d}A^* = g^* \mathrm{d}s$, $g^* = (1+\beta^2)^{-\frac{3}{2}} g$.

The formula for the potential energy generated by the initial stress is as follows:

$$\begin{aligned} U_0 &= \iint (n_0^{xx}\gamma_{xx}^{nl} + n_0^{xs}\gamma_{xs}^{nl} + n_0^{sx}\gamma_{sx}^{nl})\mathrm{d}S \\ &= \iint (n_0^{xx}\gamma_{xx}^{nl} + 2n_0^{xs}\gamma_{xs}^{nl})\mathrm{d}S, \end{aligned} \tag{17}$$

where $n_0^{xx} = E'g(1+\beta^2)^{-2}\gamma_{xx}^0$, n_0^{xs} is defined by formula (14), γ_{xx}^0 is the strain generated by the external loads, determined for the linear problem, γ_{xx}^{nl} is the nonlinear part of the strains, defined by formula (8), and γ_{xs}^{nl} is the nonlinear part of the strains, defined by formula (9).

The work of the external load is expressed as follows:

$$W = \int_a^b (\mathbf{p} \circ \mathbf{u}^p)\mathrm{d}x = \int_a^b (p_x u_x^p + p_y u_y^p + p_z u_z^p)\mathrm{d}x, \tag{18}$$

where $\mathbf{p} = [p_x, p_y, p_z]$ is the external load vector, $\mathbf{u}^p = [u_x^p, u_y^p, u_z^p]^T$ and is the vector of the displacements of the external load application points.

The components of the displacement vector $\mathbf{u}^p$ are defined by the following formulas:

$$\begin{aligned} u_x^p &= u_{ox} - y^p u_{y,x} - z^p u_{z,x} - \omega^p \theta_{,x}, \\ u_y^p &= u_y - z^p\theta - \frac{1}{2}y^p\theta^2, \\ u_z^p &= u_z + y^p\theta - \frac{1}{2}z^p\theta^2, \end{aligned} \tag{19}$$

where $[x^p, y^p, z^p]$ is the vector of the external load application point coordinates, and ω^p is the sectorial coordinate of the load application point.

As a result of the transformations performed in formula (15) and taking into account the fact that the load vector in the considered problem has the form $\mathbf{p} = [0, 0, p_z]$, one obtains a system of displacement equations. The system comprises four coupled differential equations, three of which are fourth-order equations. The equations are expressed by the following formulas:

$$E(-A^* u_{ox,x})_{,x} + \chi\left(-I^0_{\substack{y,1\\x,1}} u_{y,x} - I^0_{\substack{z,1\\x,1}} u_{z,x} - I^0_{\substack{z,2\\x,1}} u_{z,xx}\right)_{,x} = 0, \tag{20}$$

$$\begin{aligned} &E(I_z^* u_{y,xx})_{,xx} + \chi\left(\left(I^0_{\substack{\theta,1\\y,2}}\theta_{,x} + I^0_{\substack{\theta,2\\y,2}}\theta_{,xx}\right)_{,xx}\right. \\ &\left. - \left(I^0_{\substack{y,1\\x,1}} u_{ox,x} + I^0_{\substack{\theta\\y,1}}\theta + I^0_{\substack{\theta,1\\y,1}}\theta_{,x}\right)_{,x}\right) = 0, \end{aligned} \tag{21}$$

$$\begin{aligned} &E(I_y^* u_{z,xx})_{,xx} + \chi\left(\left(I^0_{\substack{z,2\\x,1}} u_{ox,x} + I^0_{\substack{\theta,1\\z,2}}\theta_{,x}\right)_{,xx}\right. \\ &\left. - \left(I^0_{\substack{z,1\\x,1}} u_{ox,x} + I^0_{\substack{\theta\\z,1}}\theta + I^0_{\substack{\theta,1\\z,1}}\theta_{,x}\right)_{,x}\right) - \chi p_z = 0, \end{aligned} \tag{22}$$

$$\begin{aligned} &E((I_\omega^*\theta_{,xx} + I_{\psi\omega}^*\theta_{,x})_{,xx} - (I_\psi^*\theta_{,x} + I_{\psi\omega}^*\theta_{,xx})_{,x} - G(I_s\theta_{,x})_{,x}) \\ &+ \chi\left(\left(I^0_{\substack{\theta,2\\y,2}} u_{y,xx}\right)_{,xx}\right. \\ &- \left(I^0_{\substack{\theta,1\\y,1}} u_{y,x} + I^0_{\substack{\theta,1\\y,2}} u_{y,xx} + I^0_{\substack{\theta,1\\z,1}} u_{z,x} + I^0_{\substack{\theta,1\\z,2}} u_{z,xx}\right)_{,x} \\ &\left. + \left(I^0_{\substack{\theta\\y,1}} u_{y,x} + I^0_{\substack{\theta\\z,1}} u_{z,x}\right)\right) - \chi\,(p_z\, y^p - p_z\, z^p\theta) = 0. \end{aligned} \tag{23}$$

The associated equations describing the boundary conditions are as follows:

$$[N\delta u_{ox}]_a^b = 0, \tag{24}$$

where

$$N = E'\left(A^* u_{ox,x} + \chi\left(I^0_{\substack{y,1\\x,1}} u_{y,x} + I^0_{\substack{z,1\\x,1}} u_{z,x} + I^0_{\substack{z,2\\x,1}} u_{z,xx}\right)\right),$$

$$[Q_y \delta u_y]_a^b = 0, \tag{25}$$

where

$$\begin{aligned} Q_y = E'\left((-I_z^* u_{y,xx})_{,x} - \chi\left(I^0_{\substack{y,1\\x,1}} u_{ox,x} + I^0_{\substack{\theta\\y,1}}\theta + I^0_{\substack{\theta,1\\y,1}}\theta_{,x}\right)\right. \\ \left. - \chi\left(I^0_{\substack{\theta,1\\y,2}}\theta_{,x} + I^0_{\substack{\theta,2\\y,2}}\theta_{,xx}\right)_{,x}\right), \end{aligned}$$

$$[M_z \delta u_{y,x}]_a^b = 0, \tag{26}$$

where

$$M_z = -E'\left(-I_z^* u_{y,xx} + \chi\left(I^0_{\substack{\theta,1\\y,2}}\theta_{,x} + I^0_{\substack{\theta,2\\y,2}}\theta_{,xx}\right)\right),$$

$$[Q_z \delta u_z]_a^b = 0, \tag{27}$$

where

$$Q_z = E'\left(-(I_y^* u_{z,xx})_{,x} + \chi\left(I^0_{\substack{z,1\\x,1}}u_{ox,x} + I^0_{\substack{\theta\\z,1}}\theta + I^0_{\substack{\theta,1\\z,1}}\theta_{,x}\right) - \chi\left(I^0_{\substack{z,2\\x,1}}u_{ox,x} + I^0_{\substack{\theta,1\\z,2}}\theta_{,x}\right)_{,x}\right),$$

$$[M_y \delta u_{z,x}]_a^b = 0, \tag{28}$$

where

$$M_y = E'\left(-I_y^* u_{z,xx} + \chi\left(-I^0_{\substack{z,2\\x,1}}u_{ox,x} - I^0_{\substack{z,2\\y,1}}u_{y,x} - I^0_{\substack{z,2\\y,2}}u_{y,xx} - I^0_{\substack{z,1\\z,1}}u_{z,x} - I^0_{\substack{z,2\\z,2}}u_{z,xx} - I^0_{\substack{\theta,1\\z,2}}\theta_{,x} - I^0_{\substack{\theta,2\\z,2}}\theta_{,xx}\right)\right),$$

$$[M_x \delta\theta]_a^b = 0, \tag{29}$$

where

$$M_x = E'((-I_\omega^*\theta_{,xx} - I_{\psi\omega}^*\theta_{,x})_{,x} + (I_\psi^*\theta_{,x} + I_{\psi\omega}^*\theta_{,xx}) - \chi\left(I^0_{\substack{\theta,1\\y,1}}u_{y,x} + I^0_{\substack{\theta,1\\y,2}}u_{y,xx} + I^0_{\substack{\theta,1\\z,1}}u_{z,x} + I^0_{\substack{\theta,1\\z,2}}u_{z,xx}\right) - \chi\left(I^0_{\substack{\theta,2\\y,2}}u_{y,xx}\right)_{,x}\Bigg) + \mathrm{GI}_s\theta_{,x},$$

$$[B\delta\theta_{,x}]_a^b = 0, \tag{30}$$

where

$$B = E'\left(I_\omega^*\theta_{,xx} + I_{\psi\omega}^*\theta_{,x} + \chi\left(I^0_{\substack{\theta,2\\y,2}}u_{y,xx}\right)\right).$$

The coefficients in formulas (20)–(30) are defined by the following formulas:

$$A^* = \int_S \mathrm{d}A^*, \quad I_y^* = \int_S z^2\,\mathrm{d}A^*, \quad I_z^* = \int_S y^2\,\mathrm{d}A^*$$
$$I_\omega^* = \int_S \omega^2\,\mathrm{d}A^*, \quad I_{\psi\omega}^* = \int_S \omega\psi\,\mathrm{d}A^*, \quad I_\psi^* = \int_S \psi^2\,\mathrm{d}A^*, \tag{31}$$

$$I^0_{\substack{q,2\\p,2}} = \int_S n_0^{xx}\alpha_{\substack{q,2\\p,2}}\mathrm{d}s^*, \quad \text{when } p, q = y,\ z,\ \theta;$$
$$I^0_{\substack{q,2\\x,1}} = \int_S n_0^{xx}\alpha_{\substack{q,2\\x,1}}\mathrm{d}s^*, \quad \text{when } q = y,\ z,\ \theta;$$
$$I^0_{\substack{x,1\\x,1}} = \int_S n_0^{xx}\alpha_{\substack{x,1\\x,1}}\mathrm{d}s^* \tag{32}$$
$$I^0_{\substack{q,j\\p,i}} = \int_S\left(n_0^{xx}\alpha_{\substack{q,j\\p,i}} + 2n_0^{xs}\zeta_{\substack{q,j\\x,i}}\right)\mathrm{d}s^* - \text{in other cases},$$
$$\mathrm{d}s^* = \sqrt{1+\beta^2}\,\mathrm{d}s.$$

4. Solution of displacement equations

The theorem given by Lewanowicz [28] was used to solve the considered problem. The theorem describes a method of solving ordinary differential equations using Gegenbauer polynomials (a detailed description of this method can be found in Lewanowicz [28] and in the present authors' publications [23–25]). Here, zero-order Gegenbauer polynomials ($\lambda = 0$), i.e. Chebyshev polynomials of the first order, were used to solve the problem,

$$T_k(x) = \sum_{m=0}^{[k/2]}(-1)^m\frac{\Gamma(k-m)}{m!(k-2m)!}(2x)^{k-2m}. \tag{33}$$

The system of differential equations being solved has the form

$$\sum_{i=0}^{n}\mathbf{P}_i(x)\,\mathbf{f}^{(i)}(x) = \mathbf{P}(x). \tag{34}$$

In the method presented by Paszkowski [29] and Lewanowicz [28], solutions are obtained in the form of the series

$$\mathbf{f}(x) = \frac{1}{2}b_0[\mathbf{f}]T_0(x) + \sum_{k=1}^{\infty}b_k[\mathbf{f}]T_k(x), \tag{35}$$

where $\mathbf{f} = [f_1 \quad f_2 \cdots f_m]^{\mathrm{T}}$, $b_k[\mathbf{f}] = [b_k[f_1] \quad b_k[f_2] \cdots b_k[f_m]]^{\mathrm{T}}$, and $b_k[f_i]$ is the kth term of the Chebyshev series expansion of the function f_i. It was shown in Lewanowicz [28] that the initial system of equations (34) is equivalent to the following system:

$$\sum_{i=0}^{n}(\mathbf{Q}_i(x)\mathbf{f}(x))^{(i)} = \mathbf{P}(x), \tag{36}$$

where the matrix $\mathbf{Q}_i(x)$ is defined by the formula

$$\mathbf{Q}_i(x) = \sum_{j=i}^{n}(-1)^{j-i}\binom{j}{j-i}(\mathbf{P}_j(x))^{(j-i)}, \quad i = 0,\ 1,\ ...,\ n. \tag{37}$$

The system of equations (36) can be reduced (see Lewanowicz [28]) to the following infinite system of equations:

$$\sum_{i=0}^{n} 2^i \sum_{m=0}^{n-i} \varrho_{nim}(k)\, b_{k-n+i+2m}[\mathbf{Q}_i(x)\,\mathbf{f}(x)] = \sum_{m=0}^{n} \varrho_{n0m}(k) b_{k-n+2m}[\mathbf{P}(x)] \quad \text{for } k \geq n, \tag{38}$$

where

$$\varrho_{ijm}(k) = (-1)^m\binom{i-j}{m}(k-i)_{j+m}(k-i+j+2m)\,(k+m+1)_{i-m}\,(k^2-i^2)^{-1},$$
$$(\alpha)_0 = 1, \quad (\alpha)_k = \alpha(\alpha+1)...(\alpha+k-1) \text{ for } k \geq 1. \tag{39}$$

The expansion coefficients $b_k[\mathbf{Q}_i(x)\,\mathbf{f}(x)]$ of the product of functions $\mathbf{Q}_i(x)\,\mathbf{f}(x)$ are calculated from the formula given below [28] under the assumption that matrices $\mathbf{Q}_i(x)$ contain exclusively polynomials. If this assumption is not satisfied, one should previously apply an appropriate approximation to the matrix $\mathbf{Q}_i(x)$:

$$b_k[x^l f(x)] = 2^{-l}\sum_{j=0}^{l}\binom{l}{j} b_{k-l+2j}[f(x)] \quad \text{for } k, l \geq 0. \tag{40}$$

When calculating coefficients with negative subscripts, one should also use the relation $b_{-k}[f] = b_k[f]$, $k > 1$.

The displacement equations describing the considered stability loss problem are differential equations of the fourth order. In this particular case (for $n = 4$), the infinite system of equations assumes the form

$$\begin{aligned}
&(k+1)(k+2)(k+3)b_{k-4}[\mathbf{Q}_0(x,\chi)\mathbf{f}(x)]\\
&-4(k^2-4)(k+3)b_{k-2}[\mathbf{Q}_0(x,\chi)\mathbf{f}(x)]\\
&+6(k^2-9)kb_k[\mathbf{Q}_0(x,\chi)\mathbf{f}(x)]\\
&-4(k^2-4)(k-3)b_{k+2}[\mathbf{Q}_0(x,\chi)\mathbf{f}(x)]\\
&+(k-1)(k-2)(k-3)b_{k+4}[\mathbf{Q}_0(x,\chi)\mathbf{f}(x)]\\
&+2(k^2-9)[(k+1)(k+2)b_{k-3}[\mathbf{Q}_1(x,\chi)\mathbf{f}(x)]\\
&-3(k-1)(k+2)b_{k-1}[\mathbf{Q}_1(x,\chi)\mathbf{f}(x)] + 3(k+1)(k\\
&-2)b_{k+1}[\mathbf{Q}_1(x,\chi)\mathbf{f}(x)]-(k-1)(k-2)b_{k+3}[\mathbf{Q}_1(x,\chi)\mathbf{f}(x)]]\\
&+4(k^2-9)(k^2-4)
\end{aligned}$$

$$\begin{aligned}
&[(k+1)b_{k-2}[\mathbf{Q}_2(x,\chi)\mathbf{f}(x)] - 2kb_k[\mathbf{Q}_2(x,\chi)\mathbf{f}(x)]\\
&+(k-1)b_{k+2}[\mathbf{Q}_2(x,\chi)\mathbf{f}(x)]] + 8(k^2-9)(k^2-4)(k^2\\
&-1)[b_{k-1}[\mathbf{Q}_3(x,\chi)\mathbf{f}(x)] - b_{k+1}[\mathbf{Q}_3(x,\chi)\mathbf{f}(x)]]\\
&+16(k^2-9)(k^2-4)(k^2-1)kb_k[\mathbf{Q}_4(x,\chi)\mathbf{f}(x)] = 0,\\
&\text{for } k \geq 4.
\end{aligned} \tag{41}$$

The system of equations describing the considered problem, formulated in the preceding section, was reduced to the following matrix form:

$$\sum_{i=0}^{4}(\mathbf{K}_i(x) + \chi\mathbf{R}_i(x))\mathbf{f}^{(i)}(x) = \mathbf{0}. \tag{42}$$

The coefficients of the stiffness matrix $\mathbf{K}_i$ and geometric stiffness matrix $\mathbf{R}_i$ are defined by the following formulas:

$$\mathbf{K}_0 = E\begin{bmatrix}0&0&0&0\\0&0&0&0\\0&0&0&0\\0&0&0&0\end{bmatrix}, \quad \mathbf{K}_1 = E\begin{bmatrix}k_{11}^1&0&0&0\\0&0&0&0\\0&0&0&0\\0&0&0&k_{44}^1\end{bmatrix},$$
$$\mathbf{K}_2 = E\begin{bmatrix}k_{11}^2&0&0&0\\0&k_{22}^2&0&0\\0&0&k_{33}^2&0\\0&0&0&k_{44}^2\end{bmatrix}, \quad \mathbf{K}_3 = E\begin{bmatrix}0&0&0&0\\0&k_{22}^3&0&0\\0&0&k_{33}^3&0\\0&0&0&k_{44}^3\end{bmatrix}, \tag{43}$$
$$\mathbf{K}_4 = E\begin{bmatrix}0&0&0&0\\0&k_{22}^4&0&0\\0&0&k_{33}^4&0\\0&0&0&k_{44}^4\end{bmatrix},$$

$$\mathbf{R}_0 = \begin{bmatrix}0&0&0&0\\0&0&0&r_{24}^0\\0&0&0&r_{34}^0\\0&0&0&r_{44}^0\end{bmatrix}, \quad \mathbf{R}_1 = \begin{bmatrix}0&r_{12}^1&r_{13}^1&0\\r_{21}^1&0&0&r_{24}^1\\r_{31}^1&0&0&r_{34}^1\\0&r_{42}^1&r_{43}^1&0\end{bmatrix},$$
$$\mathbf{R}_2 = \begin{bmatrix}0&r_{12}^2&r_{13}^2&0\\r_{21}^2&0&0&r_{24}^2\\r_{31}^2&0&0&r_{34}^2\\0&r_{42}^2&r_{43}^2&0\end{bmatrix}, \quad \mathbf{R}_3 = \begin{bmatrix}0&0&r_{13}^3&0\\0&0&0&r_{24}^3\\r_{31}^3&0&0&r_{34}^3\\0&r_{42}^3&r_{43}^3&0\end{bmatrix}, \tag{44}$$
$$\mathbf{R}_4 = \begin{bmatrix}0&0&0&0\\0&0&0&r_{24}^4\\0&0&0&0\\0&r_{42}^4&0&0\end{bmatrix}.$$

The coefficients of the stiffness matrix $\mathbf{K}_i$ and geometric stiffness matrix $\mathbf{R}_i$ are defined by the following formulas:

$$
\begin{aligned}
&k_{11}^1 = -A_{,x}^*, \quad k_{44}^1 = I_{\psi\omega,xx}^* + 2I_{\delta\omega,x}^* - I_{\psi,x}^* - \frac{G}{E}I_{s,x},\\
&k_{11}^2 = -A^*, \quad k_{22}^2 = I_{z,xx}^*, \quad k_{33}^2 = I_{y,xx}^*,\\
&k_{44}^2 = I_{\omega,xx}^* + I_{\psi\omega,x}^* + 2I_{\delta\omega}^* - I_{\psi}^* - \frac{G}{E}I_s,\\
&k_{22}^3 = 2I_{z,x}^*, \quad k_{33}^3 = 2I_{y,x}^*, \quad k_{44}^3 = 2I_{\omega,x}^*,\\
&k_{22}^4 = I_z^*, \quad k_{33}^4 = I_y^*, \quad k_{44}^4 = I_\omega^*,
\end{aligned}
\tag{45}
$$

and

$$
\begin{aligned}
&r_{24}^0 = -\left(I^{\,0}_{\theta\ y,1}\right)_{,x} \quad r_{34}^0 = -\left(I^{\,0}_{\theta\ z,1}\right)_{,x} \quad r_{44}^0 = -p_z z^p\\
&r_{12}^1 = -\left(I^{\,0}_{y,1\ x,1}\right)_{,x} \quad r_{13}^1 = -\left(I^{\,0}_{z,1\ x,1}\right)_{,x} \quad r_{21}^1 = -\left(I^{\,0}_{y,1\ x,1}\right)_{,x}\\
&r_{24}^1 = -I^{\,0}_{\theta\ y,1} - \left(I^{\,0}_{\theta,1\ y,1}\right)_{,x} + \left(I^{\,0}_{\theta,1\ y,2}\right)_{,xx}\\
&r_{31}^1 = -\left(I^{\,0}_{z,1\ x,1}\right)_{,x} + \left(I^{\,0}_{z,2\ x,1}\right)_{,xx} \quad r_{34}^1 = -I^{\,0}_{\theta\ z,1} - \left(I^{\,0}_{\theta,1\ z,1}\right)_{,x} + \left(I^{\,0}_{\theta,1\ z,2}\right)_{,xx}\\
&r_{42}^1 = I^{\,0}_{\theta\ y,1} - \left(I^{\,0}_{\theta,1\ y,1}\right)_{,x} \quad r_{43}^1 = I^{\,0}_{\theta\ z,1} - \left(I^{\,0}_{\theta,1\ z,1}\right)_{,x}\\
&r_{12}^2 = -I^{\,0}_{y,1\ x,1} \quad r_{13}^2 = -I^{\,0}_{z,1\ x,1} - \left(I^{\,0}_{z,2\ x,1}\right)_{,x}\\
&r_{21}^2 = -I^{\,0}_{y,1\ x,1} \quad r_{24}^2 = -I^{\,0}_{\theta,1\ y,1} + 2\left(I^{\,0}_{\theta,1\ y,2}\right)_{,x} + \left(I^{\,0}_{\theta,2\ y,2}\right)_{,xx}\\
&r_{31}^2 = -I^{\,0}_{z,1\ x,1} + 2\left(I^{\,0}_{z,2\ x,1}\right)_{,x} \quad r_{34}^2 = -I^{\,0}_{\theta,1\ z,1} + 2\left(I^{\,0}_{\theta,1\ z,2}\right)_{,x}\\
&r_{42}^2 = -I^{\,0}_{\theta,1\ y,1} - \left(I^{\,0}_{\theta,1\ y,2}\right)_{,x} + \left(I^{\,0}_{\theta,2\ y,2}\right)_{,xx} \quad r_{43}^2 = -I^{\,0}_{\theta,1\ z,1} - \left(I^{\,0}_{\theta,1\ z,2}\right)_{,x}\\
&r_{13}^3 = -I^{\,0}_{z,2\ x,1} \quad r_{24}^3 = I^{\,0}_{\theta,1\ y,2} + 2\left(I^{\,0}_{\theta,2\ y,2}\right)_{,x} \quad r_{31}^3 = I^{\,0}_{z,2\ x,1} \quad r_{34}^3 = I^{\,0}_{\theta,1\ z,2}\\
&r_{42}^3 = -I^{\,0}_{\theta,1\ y,2} + 2\left(I^{\,0}_{\theta,2\ y,2}\right)_{,x} \quad r_{43}^3 = -I^{\,0}_{\theta,1\ z,2}\\
&r_{24}^4 = I^{\,0}_{\theta,2\ y,2} \quad r_{42}^4 = I^{\,0}_{\theta,2\ y,2}.
\end{aligned}
\tag{46}
$$

In order to determine the multiplier χ defining the critical load, one solves the eigenproblem, limiting oneself to the "first" eigenvalue χ_{kryt} for which the matrix equation (42) has a nonzero solution $\mathbf{f}(x)$.

The obtained vector of solutions $\mathbf{f}(x)$ has the form $\mathbf{f}(x) = [u_{ox} \;\; u_y \;\; u_z \;\; \theta]^T$, where

$$
\begin{aligned}
&u_\beta(x) = \frac{1}{2}b_0[u_\beta]T_0(x) + \sum_{k=1}^{\infty} b_k[u_\beta]T_k(x), \quad \beta = ox,\ y,\ z;\\
&\theta = \frac{1}{2}b_0[\theta]T_0(x) + \sum_{k=1}^{\infty} b_k[\theta]T_k(x).
\end{aligned}
\tag{47}
$$

The above system is satisfied when $k \geq 4$ is completed with 14 equations describing the boundary conditions. When formulating the conditions, the following relations for the values of Chebyshev polynomials of the first kind and their derivatives at points $x = \mp 1$ are used:

$$
\begin{aligned}
&T_k(1) = 1,\\
&d^m T_k(x)/\mathrm{d}x^m|_{x=1} = \frac{k}{(2m-1)!!}\prod_{l=-m+1}^{m-1}(k+l),\\
&d^m T_k(x)/\mathrm{d}x^m|_{x=-1} = (-1)^{k-m}\, d^m T_k(x)/\mathrm{d}x^m|_{x=1}\ .
\end{aligned}
\tag{48}
$$

The obtained infinite system of equations, after it is cut down to a finite system ($4M$ of the first equations) assumes the form

$$
\mathbf{A}(\chi)\mathbf{b} = 0, \tag{49}
$$

where $\mathbf{A}$ is the coefficient matrix dependent on χ, $\dim\mathbf{A} = 4M \times 4M$, $\mathbf{b} = [b_0[u_{ox}],\ b_0[u_y], b_0[u_z], b_0[\theta], \ldots, b_{M-1}[u_{ox}], b_{M-1}[u_y],\ b_{M-1}[u_z],\ b_{M-1}[\theta]]^T$ is a vector of the expansion of the obtained functions describing the generalized displacements of the system, and χ is a load multiplier.

The value of the critical load multiplier χ_{kryt} resulting in stability loss is calculated from the condition

$$
\det(\mathbf{A}(\chi_{kryt})) = 0. \tag{50}
$$

After solving equations (50) and substituting $\chi = \chi_{kryt}$ into equation (49), one obtains a homogenous system of algebraic equations for determining the form of stability loss:

$$
\mathbf{A}(\chi_{kryt})\mathbf{b} = 0. \tag{51}
$$

The aim of the present study was to determine the optimal dimensions of a tapered bisymmetric thin-walled double-T cantilever, for which, at a constant mass, the critical buckling load reaches its maximum value. Optimal solutions were sought in a discrete set of admissible values of the web's and/or the double-T bar's taper coefficients.

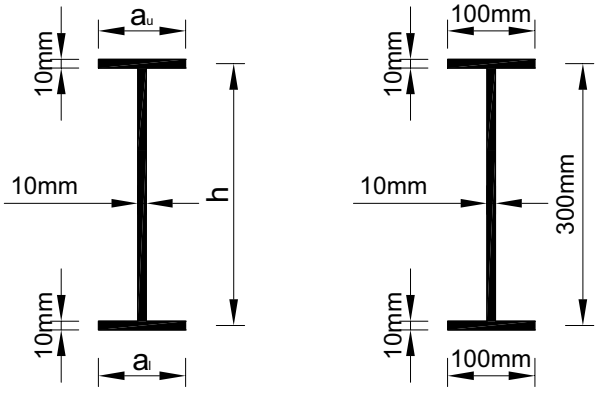

Figure 3. Cross-section at beam's midspan $x = 0$.

Source: Author's contribution.

5. Problem formulation

The aim of this research is to optimize the dimensions of a bisymmetric nonprismatic cantilever beam whose web and flanges' dimensions vary linearly along the length of the cross section and which is subjected to the action of a uniformly distributed load q (kN/m). In other words, the aim is to determine the beam's dimensions for which, at a

Ψ_f	Ψ_w									
	0.0	0.1	0.2	0.3	0.4	0.5	0.6	0.7	0.8	S_w [1]
0.0	14.77 14.77	15.72 15.72	16.76 16.71	17.88 17.73	19.10 18.79	20.43 19.90	21.90 21.05	23.58 22.24	25.50 23.47	1.73
0.1	15.75 15.74	16.72 16.79	17.79	18.94	20.21	21.60	23.15	24.91	26.92	1.71
0.2	16.67 16.67	17.66	18.73 18.97	19.91	21.20	22.63	24.23	26.04	28.07	1.68
0.3	17.55 17.54	18.53	19.60	20.78 21.31	22.08	23.53	25.15	26.96	28.97	1.65
0.4	18.38 18.34	19.34	20.39	21.56	22.86 23.78	24.29	25.89	27.66	29.60	1.61
0.5	19.18 19.05	20.12	21.15	22.29	23.54	24.93 26.31	26.46	28.14	29.99	1.56
0.6	20.03 19.67	20.93	21.92	23.00	24.19	25.49	26.91 28.79	28.47	30.21	1.51
0.7	20.99 20.14	21.84	22.75	23.75	24.85	26.04	27.34	28.94 31.04	30.43	1.45
0.8	22.04 20.43	22.81	23.65	24.56	25.57	26.67	27.89	29.26	30.72 32.79	1.39
S_f [2]	1.49	1.45	1.41	1.37	1.34	1.31	1.27	1.24	1.20	**2.08** [3]

Table 1. Critical load values when the load acts on the centre of the upper flange.

Source: Author's contribution.

[1] $S_w = \frac{q_{cr}(\psi_f = 0{,}1 * i,\quad \psi_w = 0{,}8)}{q_{cr}(\psi_f = 0{,}1 * i,\quad \psi_w = 0)}$; $i = 0,\ 1,\ \ldots,\ 8$ [2] $S_f = \frac{q_{cr}(\psi_f = 0{,}8,\quad \psi_w = 0{,}1 * j)}{q_{cr}(\psi_f = 0,\quad \psi_w = 0{,}1 * j)}$; $j = 0,\ 1,\ \ldots,\ 8$ [3] $S_{fw} = \frac{q_{cr}(\psi_f = 0{,}8,\quad \psi_w = 0{,}8)}{q_{cr}(\psi_f = 0,\quad \psi_w = 0)}$.

constant mass (volume) of the beam, the critical load causing the buckling of the beam will be maximum. Here, the term "optimization" is not used in its typical sense, i.e. as the determination of the global extremum of an objective function (the maximum critical load in this case), but as the selection of a certain "best" system from a discrete set of "admissible" systems. As an "admissible" system, the authors understand a set of cantilevers with specific characteristics. The following four types of "admissible" systems are considered:

- type W – for which an optimal system is sought in a set of cantilever beams with linearly decreasing web depth (the width of the flanges is constant),
- type F – for which an optimal system is sought in a set of cantilever beams with linearly decreasing width of the flanges (the depth of the web is constant),
- type F-W – for which an optimal system is sought in a set of cantilever beams with linearly decreasing web depth and linearly decreasing flange width (the relationship between the depth and the width is described below),
- type F_{ind}–W_{ind} – for which an optimal solution is sought in a set of cantilever beams with linearly decreasing web depth and linearly decreasing flange width (the depth and the width are independent variables).

When one denotes the taper parameter for the depth of the web, the width of the upper flange and the width of the lower flange are, respectively, ψ_w, ψ_{fu}, ψ_{fl}, where

$$\psi_w = \frac{h(0) - h(a)}{h(0)}, \quad \psi_{fu} = \frac{a_u(0) - a_u(a)}{a_u(0)}, \quad \psi_{fl} = \frac{a_l(0) - a_l(a)}{a_l(0)}. \tag{52}$$

Then, when looking for the optimal solution, one additionally assumes for sets of type F and F-W that $\psi_f = \psi_{fu} = \psi_{fl}$ and for sets of type W-F that $\psi_f = \psi_w$. Hence, the process of determining the optimal solution for a set of beams of types W, F, and F-W reduces to searching for one "optimal" design parameter ψ_w and ψ_f or $\psi_{fw} = \psi_f = \psi_w$, and in the case of a set of type F_{ind}–W_{ind}, to searching for two "optimal" design parameters ψ_w and ψ_f.

The dimensions of the midspan cross section of the considered beams are shown in Figure 3. Due to the constant volume assumption and the assumption of the linear change of the dimensions of the web and flanges, this

Ψ_f	Ψ_w									
	0.0	0.1	0.2	0.3	0.4	0.5	0.6	0.7	0.8	S_w
0.0	24.35 24.36	25.40 25.39	26.46 26.40	27.53 27.38	28.60 28.35	29.69 29.30	30.82 30.23	32.06 31.15	33.57 32.06	1.38
0.1	26.59 26.57	27.66 27.69	28.74	29.82	30.92	32.03	33.19	34.47	36.04	1.36
0.2	28.66 28.64	29.73	30.80 31.00	31.88	32.98	34.10	35.27	36.56	38.12	1.33
0.3	30.54 30.52	31.59	32.64	33.70 34.22	34.78	35.88	37.02	38.28	39.81	1.30
0.4	32.21 32.18	33.21	34.21	35.22	36.25 37.25	37.29	38.39	39.59	41.04	1.27
0.5	33.64 33.56	34.56	35.49	36.43	37.37	38.34 39.97	39.35	40.47	41.85	1.24
0.6	34.87 34.58	35.71	36.55	37.39	38.23	39.11	40.02 42.21	41.07	42.36	1.21
0.7	36.10 35.16	36.84	37.57	38.31	39.06	39.84	40.67	41.59 43.73	42.83	1.19
0.8	37.50 35.16	38.15	38.79	39.43	40.09	40.78	41.53	42.41	43.30 44.18	1.15
S_f	1.54	1.50	1.47	1.43	1.40	1.37	1.35	1.32	1.29	**1.78**

Table 2. Critical load values when the load acts on the centre of the web.

Source: Author's contribution.

Ψ_f	Ψ_w									
	0.0	0.1	0.2	0.3	0.4	0.5	0.6	0.7	0.8	S_w
0.0	33.07 33.18	34.29 34.36	35.46 35.48	36.58 36.54	37.66 37.54	38.68 38.47	39.69 39.35	40.74 40.16	42.09 40.91	1.27
0.1	36.87 36.85	38.11 38.11	39.28	40.39	41.45	42.45	43.42	44.47	45.87	1.24
0.2	40.42 40.37	41.64	42.78 42.92	43.85	44.87	45.82	46.76	47.79	49.17	1.22
0.3	43.69 43.67	44.87	45.96	46.99 47.44	47.94	48.84	49.71	50.68	52.01	1.19
0.4	46.66 46.65	47.76	48.78	49.71	50.57 51.49	51.36	52.12	53.00	54.24	1.16
0.5	49.24 49.22	50.23	51.13	51.93	52.65	53.30 54.85	53.93	54.70	55.84	1.13
0.6	51.42 51.25	52.28	53.03	53.68	54.25	54.76	55.28 57.26	55.98	57.03	1.11
0.7	53.34 52.58	54.05	54.65	55.17	55.61	56.02	56.47	56.93 58.36	58.09	1.09
0.8	55.21 52.96	55.77	56.24	56.63	56.96	57.28	57.66	58.23	58.84 57.69	1.07
S_f	1.67	1.63	1.59	1.55	1.51	1.48	1.45	1.43	1.40	**1.78**

Table 3. Critical load values when the load acts on the centre of the lower flange.

Source: Author's contribution.

cross-section does not change its dimensions in the set of "admissible" systems.

Furthermore, it was assumed that all the walls are 0.01 m thick. Under the assumptions of the linear change of the beam cross-sectional dimensions and the constant beam volume, the dimensions of the midspan cross-section and parameters ψ_w or ψ_f explicitly defined the dimensions of any cross-section of the cantilever. The sought functions were approximated with a 15-term Chebyshev series. Analyses were performed for three cases of

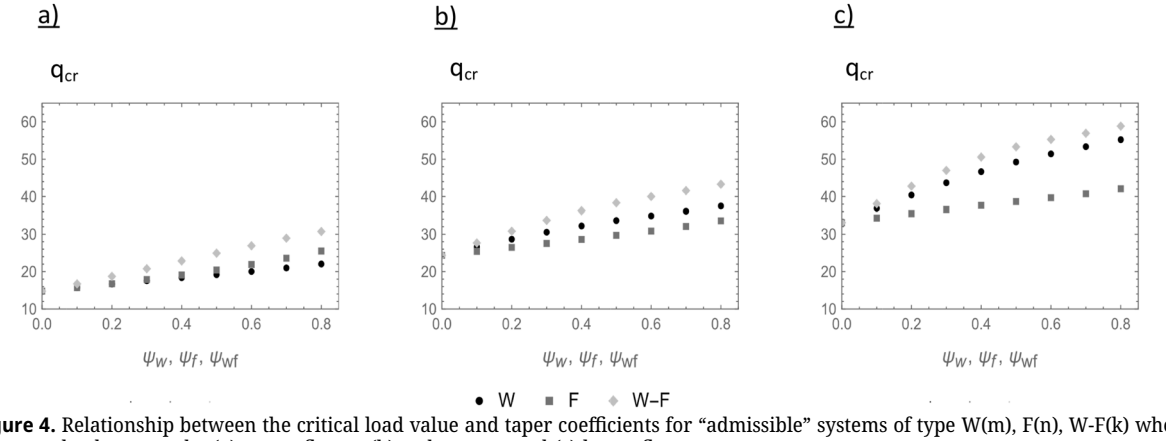

Figure 4. Relationship between the critical load value and taper coefficients for "admissible" systems of type W(m), F(n), W-F(k) when load acts on the (a) upper flange, (b) web centre, and (c) lower flange.

Source: Author's contribution.

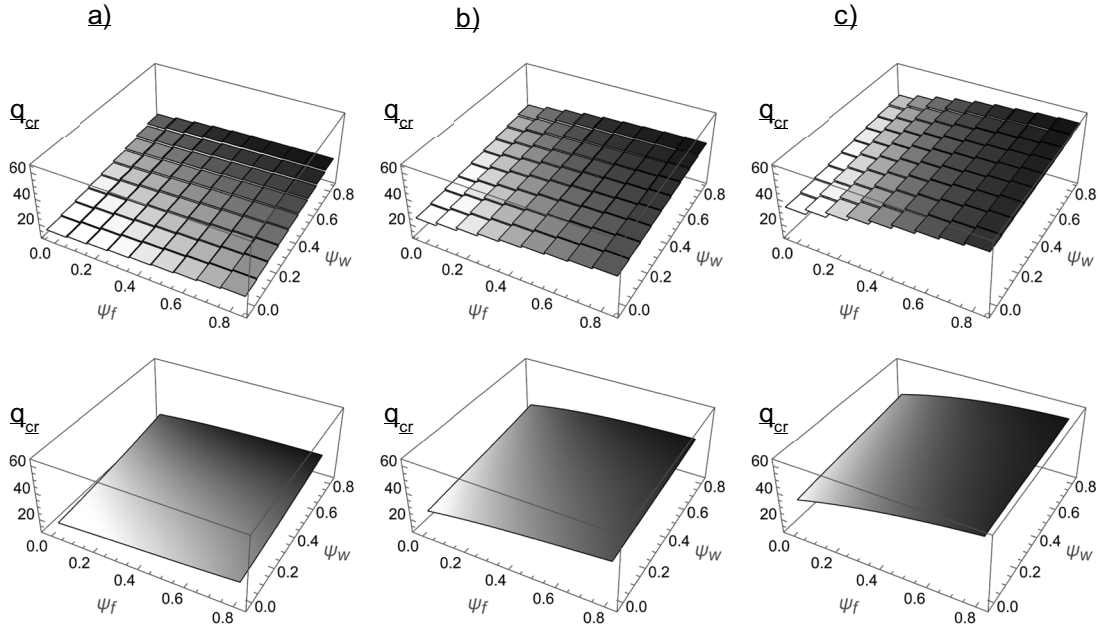

Figure 5. Relationship between the critical load value and taper coefficients for "admissible" systems W_{ind}–F_{ind} when the load acts on the (a) upper flange, (b) web centre, and (c) lower flange. Diagrams for a set of discrete values and diagrams for discrete values continuous approximation are shown in top and bottom figures, respectively.

Source: Author's contribution.

external load application: the load applied in the centre of the upper flange, in the centre of the web, and in the centre of the lower flange.

All the analysed beams had a length $L = 2a = 4$m. The material parameters of the beams were $E' = 210$ GPa, and $G = 80.77$ GPa. As already mentioned, the analyses were performed for a discrete set of dimensions defined by discrete sets of taper parameters ψ_f, ψ_w. The following values of the parameters were assumed: ψ_f, ψ_w = 0.0, 0.1, 0.2, 0.3, 0.4, 0.5, 0.6, 0.7, 0.8. The obtained values of the critical buckling load are presented in Tables 1–3. The results in Table 1 are for the case when the load acts on the centre of the upper flange. The results in Tables 2 and 3 are for the case when the load acts on the centre of the web and on the centre of the lower flange, respectively. In order to verify the results obtained using the method presented in this article, they were compared with the critical load values calculated using the FEM and Sofistik. The cantilever was approximated with 50 finite prismatic bar elements. The calculations in Sofistik were limited to three "admissible" systems, i.e. W, F, and W-F. The results obtained by FEM are presented in Tables 1–3. The following convention of presenting the results was observed: in the table cells where there are two critical load values, i.e. vP/vF, vP refers to the value determined by the method presented in this article, whereas vF refers to the value determined using FEM. As mentioned earlier, calculations were performed for a discrete set of web and/or flange taper parameters. Graphs of critical load as a function of parameters ψ_f and/or ψ_w for three cases differing in their application points are presented in Figures 4 and 5. Figure 4 shows the relationship between the critical load and taper coefficients for "admissible" systems of types W, F, and W-F. This relationship for an "admissible" system of type W_{ind}–F_{ind} is shown in Figure 5, where, besides critical load, graphs for a discrete set of parameters, also graphs of critical load as a continuous function of the parameters, are presented. The continuous critical load functions were obtained by approximating the discrete set of results with a polynomial of two third-degree variables ψ_f and ψ_w. All the calculations and the function graphs were made using *Mathematica 14* [30].

6. Analysis of results

An analysis of the results shows that for all the considered types of systems, the optimal (highest) critical buckling load value is obtained for the cantilevers with the highest taper coefficients (the largest width/height at the support, and the smallest width/height of the free end). The ratio of the optimal critical load value to the critical load value for a prismatic beam amounts to, respectively, the following:

– type W – 1.73 (variation range: 14.77–25.50 kN/m),
– type F – 1.49 (variation range: 14.77–22.04 kN/m),
– types W-F and W_{ind}–F_{ind} – 2.08 (variation range: 14.77–30.72 kN/m)
when a uniformly distributed load acts in the centre of the upper flange,
– type W – 1.38 (variation range: 24.35–33.57 kN/m),
– type F – 1.49 (variation range: 24.35–37.50 kN/m),
– types W-F and W_{ind}–F_{ind} – 1.78 (variation range: 24.35–43.30 kN/m)
when a uniformly distributed load acts in the centre of the web,
– type W – 1.27 (variation range: 33.07–42.09 kN/m),
– type F – 1.49 (variation range: 33.07–55.21 kN/m),
– types W-F and W_{ind}–F_{ind} – 2.08 (variation range: 33.07–58.84 kN/m) when a uniformly distributed load acts in the centre of the lower flange.

The obtained results confirm the fact that the critical load causing buckling increases as the load application points are lowered. In the case when the load acts in the centre of, respectively, the upper flange, the web, and lower flange, the critical load ratios are 1.00: 1.65: 2.24. For the "optimal" beam, the ratios assume the values 1.00: 1.41: 1.92. One might intuitively expect that as the system's taper parameters ψ_f and ψ_w increased, and as the stiffness of the half of the beam (on its free end side) decreased, the critical load value would decrease. The presented results show that in this case, the critical load value increases, i.e. the cantilever's "stronger" part (at the fixed end) contributes considerably more to an increase in the critical load than its "weaker" part (at the free end).

7. Conclusions

The following conclusions emerge from the above analyses:

- The model presented in this article and the method used to solve the equations describing the model yield correct "exact" results already for a small approximation base (4 × 15 = 60). In order to obtain similar results using FEM, the bar was approximated with 50 finite elements. Considering the fact that each element has 14 degrees of freedom, the approximation base in FEM is about six times larger and has about 350 coordinates.
- The obtained results confirm the well-known fact that the lower the load is applied to the beam, the higher the value of the critical buckling load.
- The results show that in the case of cantilever beams with a linearly variable double-tee cross section, the optimal (i.e. the highest) value of the critical buckling load (at a constant mass) is obtained for cantilevers with the highest taper coefficients (the largest width/height at the support, and the smallest width/height of the free end).

Funding information

Authors state no funding involved.

Author contributions

Both authors contributed equally to the manuscript.

Conflict of interest statement

Authors state no conflict of interest.

References

[1] Andrade, A., Camotim, D. (2005). Lateral-torsional buckling of singly symmetric tapered beams: Theory and applications. *Journal of Engineering Mechanics*, *131*(6), 586–597. doi: 10.1061/(ASCE)0733-9399(2005)131:6(586).

[2] Benyamina, A.B., Meftah, S.A., Mohri, F., Daya, E.M. (2013). Analytical solutions attempt for lateral torsional buckling of doubly symmetric web-tapered I-beams. *Engineering Structures*, *56*, 1207–1219. doi: 10.1016/j.engstruct.2013.06.036.

[3] Andrade, A., Camotim, D., Dinis, P.B. (2007). Lateral-torsional buckling of singly symmetric web-tapered thin-walled I-beams: 1D model vs. shell FEA. *Computers & Structures*, *85*(17–18), 1343–1359. doi: 10.1016/j.compstruc.2006.08.079.

[4] Asgarian, B., Soltani, M., Mohri, F. (2013). Lateral-torsional buckling of tapered thin-walled beams with arbitrary cross-sections, *Thin-Walled Structures*, *62*, 96–108. doi: 10.1016/j.tws.2012.06.007.

[5] Branford, M.A. (1989). Inelastic buckling of tapered monosymmetric I-beams. *Engineering Structures*, *11*(2), 119–126. doi: 10.1016/0141-0296(89)90021-7.

[6] Challamel, N., Andrade, A., Camotim, D. (2007). An analytical study on the lateral-torsional buckling of linearly tapered cantilever strip beams. *International Journal of Structural Stability and Dynamics*, *7*(3), 441–456. doi: 10.1142/S0219455407002368.

[7] Osmani, A., Meftah, S.A. (2018). Lateral buckling of tapered thin walled bi-symmetric beams under combined axial and bending loads with shear deformations allowed. *Engineering Structures*, *165*(15), 76–87. doi: 10.1016/j.engstruct.2018.03.009.

[8] Raftoyiannis, I.G., Adamakos, T. (2010). Critical lateral-torsional buckling moments of steel web-tapered I-beams. *The Open Construction and Building Technology Journal*, *4*, 105–112. doi: 10.2174/1874836801004010105.

[9] Rezaiee-Pajand, M., Masoodi, A.R., Alepaighambar, A. (2018). Lateral-torsional buckling of functionally graded tapered I-beams considering lateral bracing. *Steel and Composite Structures*, *28*(4), 403–414. doi: 10.12989/scs.2018.28.4.403.

[10] Soltani, M. (2022). A novel approach for lateral buckling assessment of double tapered thin-walled laminated composite I-beams. *Mechanics of Advanced Composite Structures*, *9*, 11–23. doi: 10.22075/macs.2021.22105.1313.

[11] Soltani, M., Asgarian, B. (2021). Exact stiffness matrices for lateral–torsional buckling of doubly symmetric tapered beams with axially varying material properties. *Iranian Journal of Science and Technology, Transactions of Civil Engineering*, *45*, 589–609. doi: 10.1007/s40996-020-00402-z.

[12] Soltani, M., Asgarian, B. (2020). Lateral-torsional stability analysis of a simply supported axially functionally graded beam with a tapered I-section. *Mechanics of Composite Materials*, *56*, 39–54. doi: 10.1007/s11029-020-09859-5.

[13] Soltani, M., Asgarian, B., Mohri, F. (2019). Improved finite element model for lateral stability analysis of axially functionally graded nonprismatic I-beams. *International Journal of Structural Stability and Dynamics*, *19*(9), 1950108. doi: 10.1142/S0219455419501086.

[14] Soltani, M., Gharebaghi, S.A., Mohri, F. (2018). Lateral stability analysis of steel tapered thin-walled beams under various boundary conditions. *Journal of Numerical Methods in Civil Engineering*, *3*(1), 13–25. doi: 10.29252/nmce.3.1.13.

[15] Zhang, L., Tong, G.S. (2008). Lateral buckling of web-tapered I-beams: A new theory. *Journal of Constructional Steel Research*, *64*(12), 1379–1393. doi: 10.1016/j.jcsr.2008.01.014.

[16] El-Mahdy, G.M., El-Saadawy, M.M. (2015). Ultimate strength of singly symmetrical I-section steel beams with variable flange ratio. *Thin-Walled Structures*, *87*, 149–157. doi: 10.1016/j.tws.2014.11.016.

[17] Ruta, P. (1999). Application of Chebyshev series to solution of non-prismatic beam vibration problems. *Journal of Sound and Vibration*, *227*(2), 449–467. doi: 10.1006/jsvi.1999.2348.

[18] Ruta, P. (2002). Dynamic stability problem of non-prismatic rod. *Journal of Sound and Vibration*, *250*(3), 445–464. doi: 10.1006/jsvi.2001.3954.

[19] Ruta, P. (2006). The application of Chebyshev polynomials to the solution of the nonprismatic Timoshenko beam vibration problem. *Journal of Sound and Vibration*, *296*(1–2), 243–263. doi: 10.1016/j.jsv.2006.02.011.

[20] Ruta, P., Szybiński, J. (2014). Free vibration of non-prismatic sandwich beams using the Chebyshev series. *Procedia Engineering*, *91*, 105–111. doi: 10.1016/j.proeng.2014.12.022.

[21] Ruta, P., Szybiński, J. (2015). Lateral stability of bending non-prismatic thin-walled beams using orthogonal series. *Procedia Engineering*, *111*, 694–701. doi: 10.1016/j.proeng.2015.07.134.

[22] Ruta, P., Szybiński, J. (2015). Nonlinear analysis of nonprismatic Timoshenko beam for different geometric nonlinearity models. *International Journal of Mechanical Sciences*, *101–102*, 349–362. doi: 10.1016/j.ijmecsci.2015.07.020.

[23] Szybiński, J., Ruta, P. (2021). An analysis of the effect of a change in the support point location on the vibration of thin-walled beams. *International Journal of Structural Stability and Dynamics*, *21*(9), 2150125. doi: 10.1142/S021945542150125X.

[24] Szybiński, J., Ruta, P. (2019). Analysis of thin-walled beams with variable monosymmetric cross section by means of Legendre polynomials. *Studia Geotechnica et Mechanica*, *41*(1), 1–12. doi: 10.2478/sgem-2019-0001.

[25] Szybiński, J., Ruta, P. (2022). Effect of a “slight” curvature of the axis of a thin-walled nonprismatic beam on its free vibration. *International Journal of Structural Stability and Dynamics*, *22*(7), 2250043. doi: 10.1142/S0219455422500432.

[26] SOFiSTiK v2024. (2024). *User’s Manuals. SOFISTIK AG*. Oberschleissheim, Germany.

[27] Wilde, P. (1968). The torsion of thin-walled bars with variable cross-section. *Archives of Mechanics*, *4*(20), 431–443.

[28] Lewanowicz, S. (1976). Construction of a recurrence relation of the lowest order for coefficients of the Gegenbauer series. *Applicationes Mathematicae*, *15*(3), 345–396.

[29] Paszkowski, S. (1975). *The numerical application of Chebyshev polynomials and series (in Polish)*. Warsaw: Polish Scientific Publishers.

[30] Wolfram Research, Inc., Mathematica, Version 14.0, Champaign, IL (2023).